

Supporting Information for

Selective C–H Bond Cleavage by a High Spin Fe^{IV}–Oxido Complex

Chen Sun, Jennifer L. Jaimes, Alec H. Follmer, Joseph W. Ziller, and A.S. Borovik*

Table of Contents

Figure S1. Zoomed in electronic absorption spectrum of [Fe ^{IV} pop(O)] [−] .	S2
Figure S2. Electronic absorption spectrum of the reaction of [Fe ^{IV} pop(O)] [−] with BzOH and the corresponding pseudo first-order kinetic plots.	S2
Figure S3. Plot of k_{obs} vs. the concentration of BzOH.	S3
Figure S4. Plot of k_{obs} vs. the concentration of [Fe ^{IV} pop(O)] [−] .	S3
Figure S5. Plot of k_{obs} vs. the concentration of 4-R-BzOH and the corresponding Hammett plot.	S4
Figure S6. GCMS data for the reaction of [Fe ^{IV} pop(O)] [−] with BzOH (1:1).	S4
Figure S7. ¹ H NMR spectra comparing benzaldehyde to the extracted organic S4 product from the reaction of [Fe ^{IV} pop(O)] [−] with and without BzOH.	S5
Figure S8. Plot of k_{obs} vs. the concentration of BzOMe.	S5
Figure S9. Plot of k_{obs} vs. the concentration of BzOH using either [Fe ^{IV} pop(O)] [−] or [Fe ^{IV} poat(O)] [−] as the oxidant.	S6
Scheme S1. Expression for the proposed pre-equilibrium between [Fe ^{IV} pop(O)] [−] and substrate.	S6
Table S1. Second order rate constants and the corresponding substituent constant for <i>para</i> -substituted benzyl alcohols.	S7
Table S2. Crystallographic Information for {K[Fe ^{II} pop(OH ₂)]} ₂ .	S7

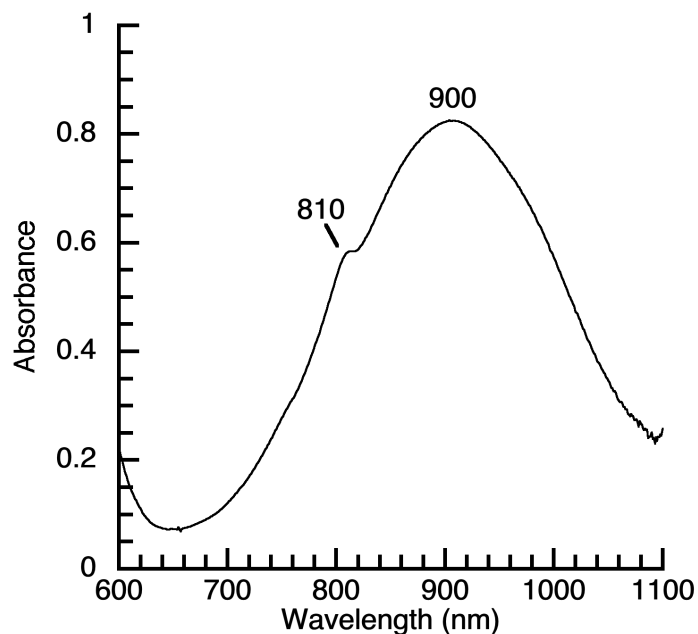


Figure S1. Electronic absorption spectrum of $[\text{Fe}^{\text{IV}}\text{pop}(\text{O})]^-$ generated using 9.23 mM $\text{K}[\text{Fe}^{\text{II}}\text{pop}(\text{OH}_2)]$ in the presence of 2.08 equiv of 18c6 + 1.06 equiv of IBX-*i*Pr in DMF:THF at -80°C , highlighting the low-energy region.

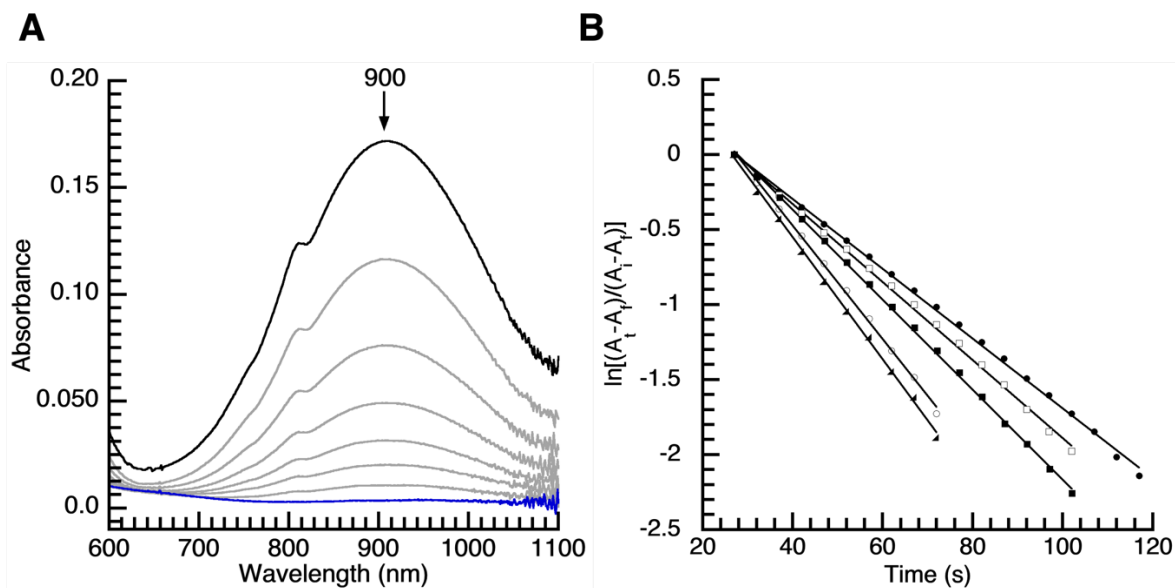


Figure S2. (A) Electronic absorption spectrum showing the disappearance of the 900 nm $d-d$ band from the reaction of $[\text{Fe}^{\text{IV}}\text{pop}(\text{O})]^-$ (1.9 mM) and BzOH under pseudo first-order rate conditions in DMF at -20°C . (B) The corresponding plot of $\ln\left(\frac{A_t - A_f}{A_i - A_f}\right)$ vs. time associated with the disappearance of the 900 nm $d-d$ band for different concentrations of BzOH.

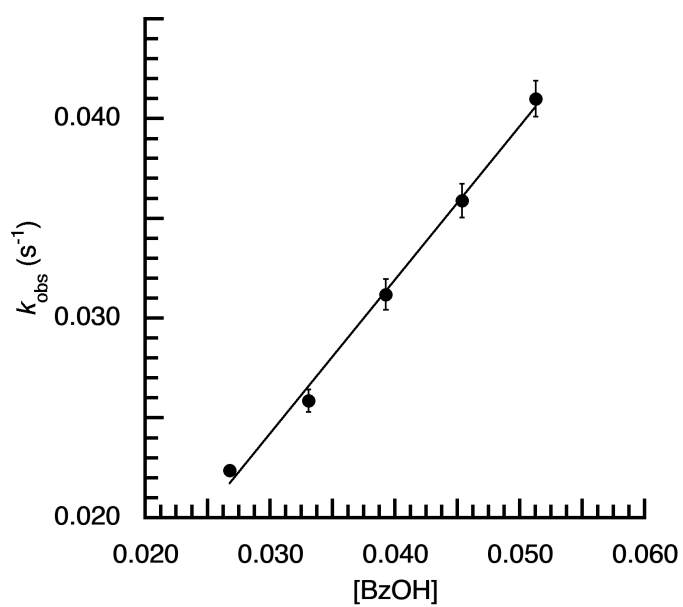


Figure S3. Plot of k_{obs} vs. the concentration of benzyl alcohol in DMF at $-20\text{ }^{\circ}\text{C}$.

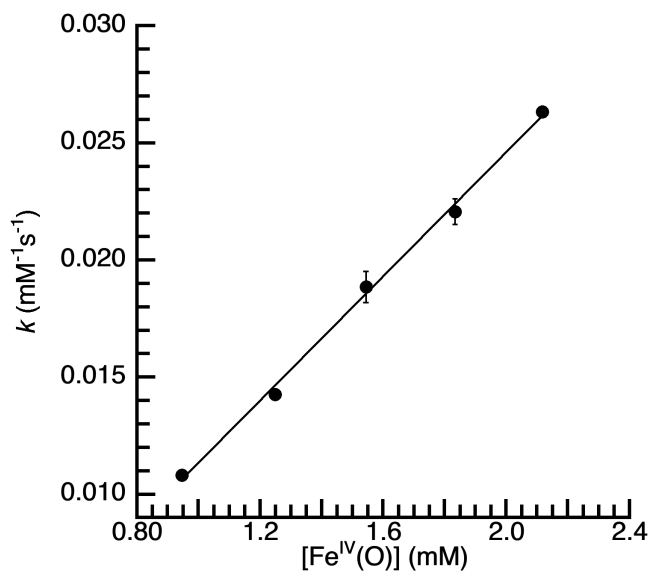


Figure S4. Plot of k vs. the concentration of $[\text{Fe}^{\text{IV}}\text{pop}(\text{O})]^{-}$ in DMF at $-20\text{ }^{\circ}\text{C}$.

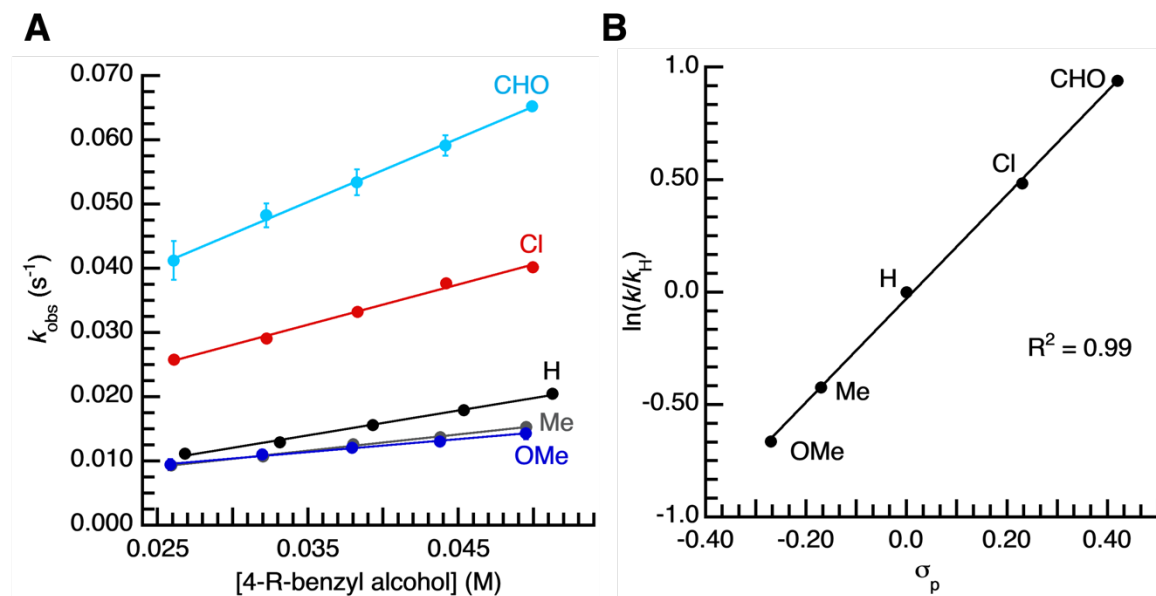


Figure S5: (A) Plot of k_{obs} vs. the concentration of 4-R-BzOH in DMF at $-20\text{ }^{\circ}\text{C}$ and (B) the corresponding Hammett plot.

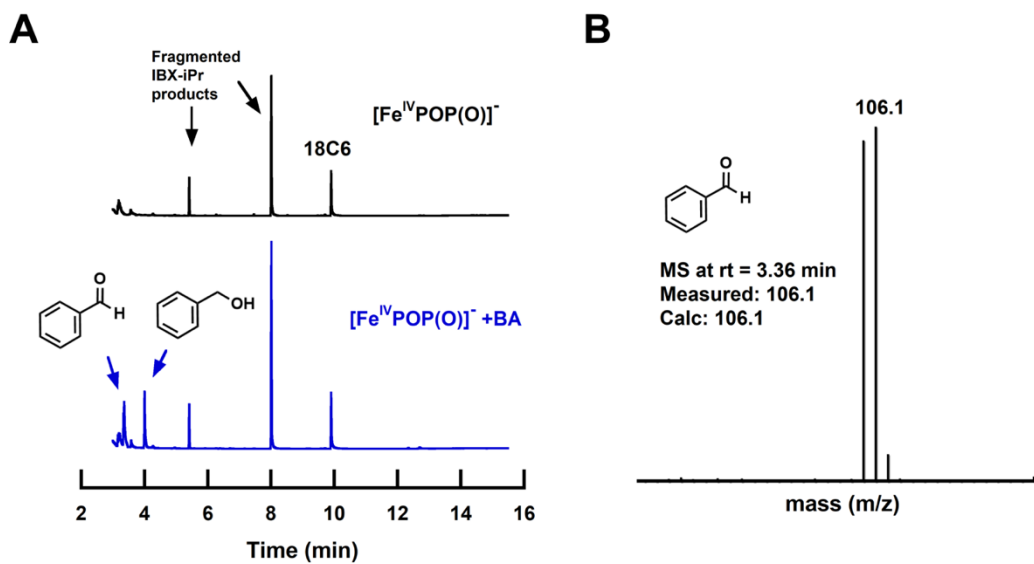


Figure S6. (A) Gas chromatograph of the organic products from the reaction of $[\text{Fe}^{\text{IV}}\text{pop}(\text{O})]^-$ with BzOH (1:1) and (B) the corresponding mass spectrum at retention time (rt) 3.36 min in CH_2Cl_2 .

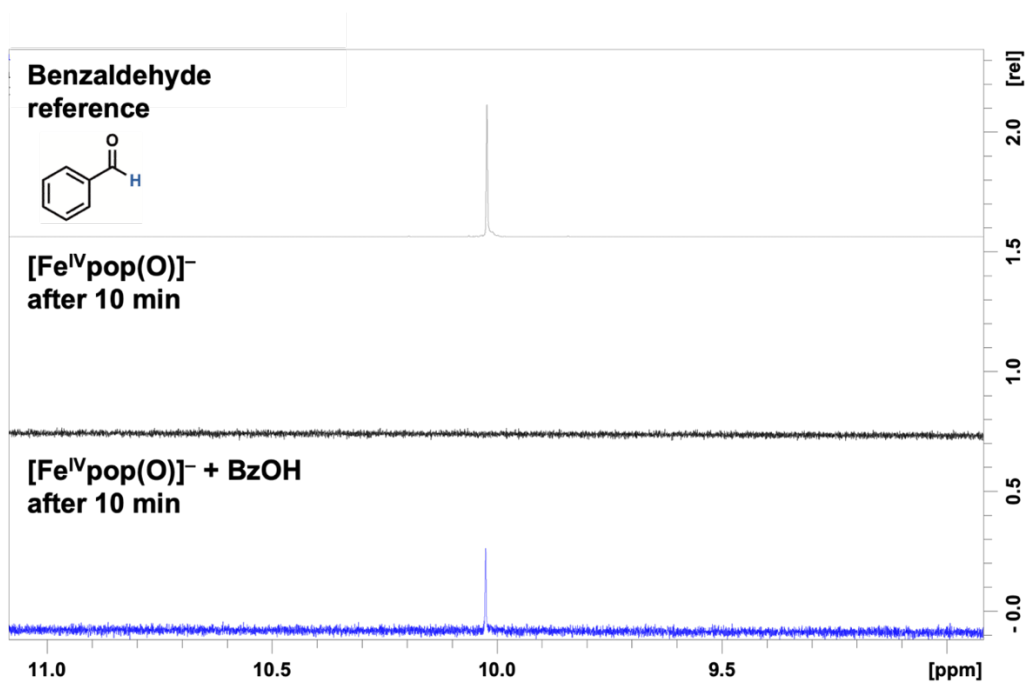


Figure S7. ¹H NMR spectrum in *d*₆-DMSO of an authentic sample of benzaldehyde (grey), the extracted organic product from the reaction of [Fe^{IV}pop(O)]⁻ without BzOH (black), and the extracted organic product from the reaction of [Fe^{IV}pop(O)]⁻ with BzOH (1:1) (blue).

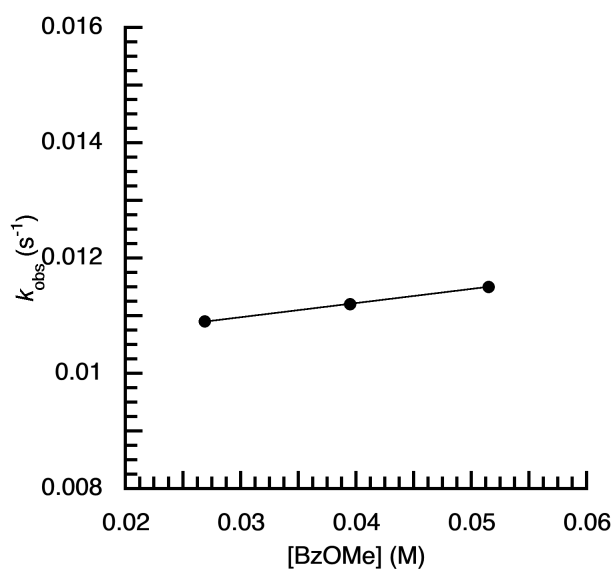


Figure S8. Plot of k_{obs} vs. the concentration of BzOMe in DMF at -20°C .

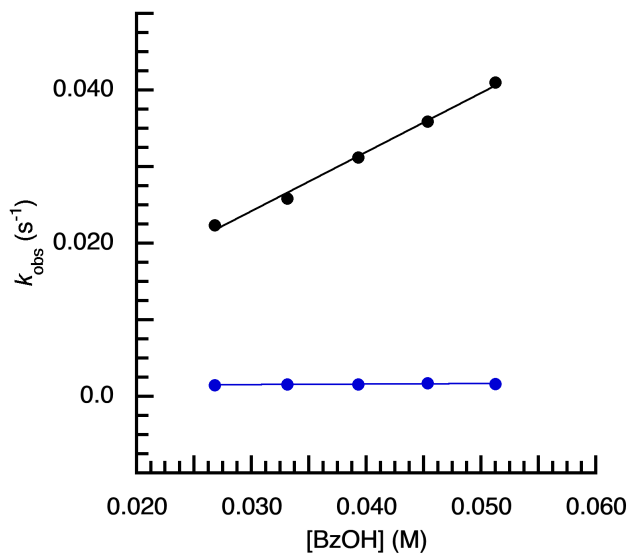
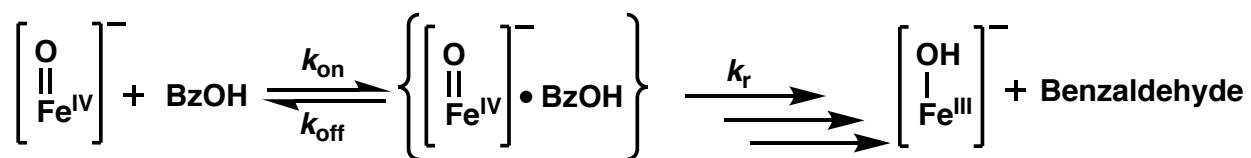


Figure S9. Plot of k_{obs} vs. the concentration of BzOH in DMF at $-20\text{ }^{\circ}\text{C}$ using either $[\text{Fe}^{\text{IV}}\text{pop}(\text{O})]^-$ (black) or $[\text{Fe}^{\text{IV}}\text{pop}(\text{O})]^-$ or $[\text{Fe}^{\text{IV}}\text{poat}(\text{O})]^-$ (blue) as the oxidant.



Scheme S1. Expression for the proposed pre-equilibrium between the Fe^{IV} -oxido complex and substrate.

Table S1. Second order rate constants (k) and the corresponding substituent constant (σ) for each respective *para*-substituted benzyl alcohol.

R	k (M⁻¹s⁻¹)	σ
OMe	0.100	-0.27
Me	0.127	-0.17
H	0.193	0
Cl	0.314	0.23
CHO	0.495	0.42

Table S2. Crystallographic Information for {K[Fe^{II}pop(OH₂)]}₂

Complex	{K[Fe^{II}pop(OH₂)]}
Empirical Formula	C ₈₄ H ₈₆ Fe ₂ K ₂ N ₈ O ₂₀ P ₆
Fw	1903.32
T (K)	133(2)
Crystal System	Triclinic
Space Group	$P\bar{1}$
a (Å)	14.427(3)
b (Å)	16.428(3)
c (Å)	20.699(4)
α (°)	99.145(2)
β (°)	98.055(2)
γ (°)	111.423(2)
V (Å ³)	4402.8(13)
Z	2
δ_{calcd} (Mg/m ³)	1.436
GOF on F ²	1.038
R1	0.0392
wR2	0.1080